The effect of excitation light source and humidity to photocatalytic activity of g-C$_3$N$_4$ nanosheets for NO removal

Tran Hoang The Vinh[1,2], Huynh Cam Tu[1,2], Pham Van Viet[1,2,*]

[1]*Faculty of Materials Science and Technology, University of Science, VNU-HCM, 227 Nguyen Van Cu Street, District 5, Ho Chi Minh City, 700000, Vietnam*

[2]*Vietnam National University-Ho Chi Minh City, Linh Trung Ward, Thu Duc District, Ho Chi Minh City, 700000, Vietnam*

Correspondence

Pham Van Viet, Faculty of Materials Science and Technology, University of Science, VNU-HCM, 227 Nguyen Van Cu Street, District 5, Ho Chi Minh City, 700000, Vietnam
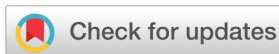
Vietnam National University-Ho Chi Minh City, Linh Trung Ward, Thu Duc District, Ho Chi Minh City, 700000, Vietnam

Email: pvviet@hcmus.edu.vn

Check for updates

VNU-HCM Press

ABSTRACT

Introduction: Photocatalysis using nanostructured semiconductors is the potential strategy to solve the problem of environmental pollution. Besides traditional semiconductor materials, the novel polymeric metal-free semiconductor g-C$_3$N$_4$ has emerged as a potential substitute material because of its many outstanding features. **Methods**: This study successfully synthesized two dimensions (2D)-structured g-C$_3$N$_4$ nanosheets by a simple thermal-exfoliation method with annealing route at 2 ^{o}C/min. Firstly, melamine was placed in a ceramic crucible with cover and then undergone the annealing route at 550 ^{o}C for 2 h to develop into the g-C$_3$N$_4$ bulk. Then the as-synthesized g-C$_3$N$_4$ bulk was further annealed without the cover at 550 ^{o}C for 2 h to form the final product, g-C$_3$N$_4$ nanosheets. **Results**: The results of XRD patterns and FTIR spectra show two typical diffraction peaks and chemical bonds that characterize the g-C$_3$N$_4$ matrix. The TEM images demonstrated that the as-prepared g-C$_3$N$_4$ possesses 2D-structured material, including several singly exfoliated sheets with a width of around several hundred nanometers. The photocatalytic NO removal efficiency of g-C$_3$N$_4$ nanosheets is highest at 48.27% under 30 min solar irradiation at 70% humidity. Meanwhile, the NO$_2$ conversion yield is very low, only 9.44%, much smaller than the NO decomposition efficiency to form NO$_3^-$ ion products. The results of trapping tests indicated that the hole plays the most critical role in the photocatalytic process of g-C$_3$N$_4$ nanosheets. Especially, the photocatalytic NO removal efficiency still achieves 45.03% after the recycling test. Moreover, all characteristic peaks and chemical bonds in material remain even undergoing fifth times reuse as the results of XRD and FTIR. **Conclusion**: From various modern analytic characterization methods and photocatalytic investigation, we can conclude that g-C$_3$N$_4$ nanosheets are very stable and possible to apply in practical applications to decompose NO gas at atmospheric conditions.

Key words: g-C3N4 nanosheets, NO removal, solar irradiation, thermal-exfoliation method

INTRODUCTION

In recent years, the accelerating pace of industrialization, modernization, and population explosion has harmed the environment due to the emissions of greenhouse gases such as NO, NO$_2$, SO$_2$, CO, CO$_2$ from means of transportation, industrial zones, factories, etc.[1]. Among them, NO is one of the most toxic gases emitted mainly from vehicles and partly from natural phenomena such as volcanic explosions, thunderstorms[2,3]. Moreover, the high concentration of NO gas in the atmosphere will negatively impact the environment causing smog formation, photochemical smog, and reaction with O$_3$ to puncture the ozone layer[4]. Especially, NO gas will directly affect human health, causing diseases of the liver, respiratory system, blood vessels, etc.[1,4,5].

To solve this problem, many research groups worldwide have spent a lot of effort in researching to remove NO gas from the air by methods such as electrostatic air purification, chemical oxidation, wet collectors, physical treatment, biological, and photocatal-

ysis[5]. Therein, the photocatalytic method using the nanostructured semiconductor material has emerged rapidly as an inexpensive, efficient, and environmentally friendly method that can decompose contaminants at high concentrations[5–7]. For instance, TiO$_2$, ZnO, SnO$_2$ are traditional semiconductors that have been widely studied in the photocatalytic field for many decades. Still, most of them are limited by a few factors such as large bandgap, small specific surface area, complicated synthesis method that have restricted the applicability of the photocatalytic method[5,8,9]. Recently, the novel material graphitic carbon nitride (g-C$_3$N$_4$) has been widely studied and known as a polymeric metal-free semiconductor for use in photocatalytic fields such as wastewater treatment, water-splitting, and pollutant gas treatment[10]. Thanks to the superior properties of the large specific surface area and narrow bandgap of about 2.7 eV, the photocatalytic ability of the g-C$_3$N$_4$ is significantly improved[10]. Especially, the morphology of g-C$_3$N$_4$ in 2D-structured nanosheets can optimize

the effective area of the photocatalyst that facilitates the reactions between the incident light and the surface of the photocatalyst. In addition, the fabrication of 2D material is feasible because the C-N bond to form g-C_3N_4 sheets is the covalent bond that is much stronger than the van der Waals weak physical bond between the sheets[10,11]. There are many ways to synthesize g-C_3N_4 nanosheets, such as physical method, chemical method with acid or base solvents, ultrasonic exfoliation, etc. However, most of these methods require expensive facilities and are not environmentally friendly because of using acid and base solvents[11]. To overcome this problem, the thermal-exfoliation process is an optimal strategy to form g-C_3N_4 nanosheets while ensuring environmental safety factors.

In this study, we synthesize g-C_3N_4 nanosheets by a simple thermal-exfoliation method. First, these modern analytical methods, such as X-ray diffraction (XRD), Fourier transform infrared (FTIR) spectroscopy, transmission electron microscopes (TEM), and UV-Vis diffuse reflectance spectroscopy (DRS) are used to investigate the properties of the material. Then, the g-C_3N_4 nanosheets are evaluated for the photocatalytic NO removal ability at 500 ppb (part per billion) of concentration under various conditions of irradiation and humidity to find the optimal condition to evaluate the applicability in Vietnam. In addition, the trapping tests are conducted to elucidate the main factor that contributes to the photocatalytic process of g-C_3N_4 nanosheets. Moreover, we also conduct recycling experiments to evaluate the practical applicability of the materials. Finally, a photocatalytic mechanism based on the g-C_3N_4 nanosheets is proposed and described concretely from the results obtained.

MATERIALS-METHODS

Chemicals and materials

All chemicals were analytical grade reagents and used as received without further purification. Melamine ($C_3H_6N_6$, 99.99%), potassium iodide (KI, 99.99%), potassium dichromate ($K_2Cr_2O_7$, 99.99%), p-benzoquinone (BQ, $C_6H_4O_2$, 99.99%), and deionized water (DI) is extracted from the Puris Evo-UP Water System.

The synthesis procedure of the materials

The g-C_3N_4 nanosheets were fabricated by the straightforward thermal-exfoliation method. Detailly, 1 g melamine was placed in a ceramic crucible with cover and then undergone the annealing route at 550 ^oC for 2 h to develop into the g-C_3N_4 bulk. Then the as-synthesized g-C_3N_4 bulk was further annealed without the cover at 550 ^oC for 2 h to form the final product, g-C_3N_4 nanosheets. The ramping rate of the annealing route is 2 ^oC/min. The whole material synthesis process was illustrated in detail, as shown in **Scheme 1**.

Characterizations of materials

The various modern analytical techniques have been applied, such as X-ray diffraction (XRD, using a Bruker D8, Advance 5005 with Cu Kα radiation (k = 0.154064 nm)), Fourier transforms infrared (FTIR) spectroscopy (Jasco V- 4700 spectrometer), transmission electron microscopes (TEM, JEM 2100, JEOL, Japan), and UV-Vis diffuse reflectance spectroscopy (DRS, JASCO-V550) to investigate the properties of materials. Therein, phase composition, chemical bonds, morphology, and optical properties of the materials are surveyed by XRD, FTIR, TEM, and DRS, respectively. Furthermore, for evaluating the photocatalytic activity of g-C_3N_4 nanosheets for NO removal, we conducted the measurement procedure as our previous study under different excitation light sources listed as shown in **Table 1**[12]. In addition, the calculation formula of photocatalytic NO removal efficiency, NO_2 conversion, NO oxidation efficiency into green products, and kinetic reaction rate k value was explicitly presented in our previous works[8,12]. Moreover, we also experimented with different humidity conditions (70%, 40%, and 20%) to deeply investigate the photocatalytic activity of g-C_3N_4 nanosheets. In addition, the trapping experiments were also performed in the same procedure as the photocatalytic activity experiment but with the presence of some trappers such as KI (h^+), $K_2Cr_2O_7$ (e^-), and BQ ($^\bullet O_2{}^-$) to clarify key factors in the photocatalytic process.

RESULTS

Figure 1a clearly shows two strong peaks located at 13.2^o and 27.4^o of the g-C_3N_4 nanosheets pattern. In **Figure 1**b, FTIR spectra reveal a marked change in the region from 1700 to 500 cm^{-1} after undergoing a thermal-exfoliation process of melamine precursor. TEM images (**Figure 2**a-b) with different magnifications showed that the morphology of the g-C_3N_4 is a 2D-structured material including several singly exfoliated sheets with a width of around several hundred nanometers. In addition, we further measure and compare the bandgap of g-C_3N_4 material using the UV-Vis DRS method.**Figure 3** indicated that the bandgap of g-C_3N_4 bulk and g-C_3N_4 nanosheets is 2.65 eV and 2.77 eV, respectively. The results clearly

Table 1: Detailed parameters of the excitation light sources

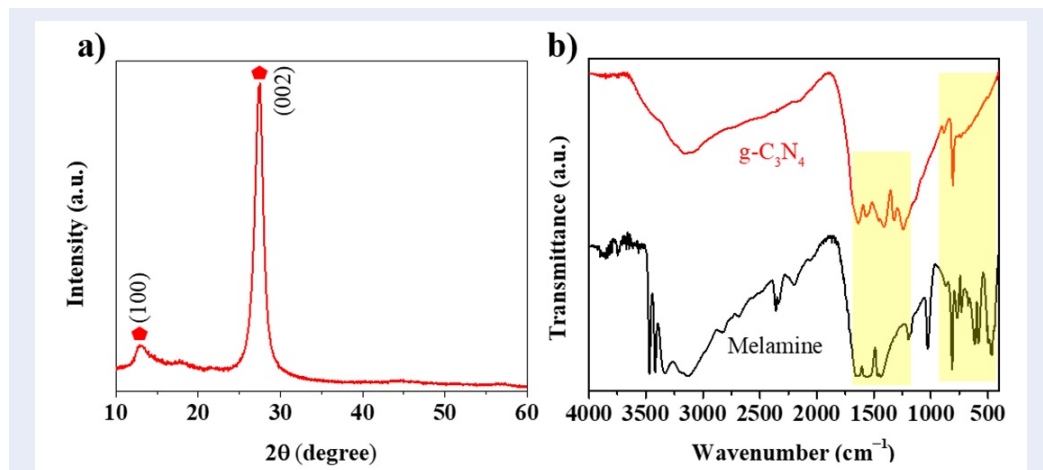| Notation of exciting light sources	Manufacturer	Power (W)	Wavelength (nm)
Solar-OSRAM	OSRAM, Germany	300	280 – 750
Vis-OSRAM	OSRAM, Germany	300	380 – 750
Solar-ABET	ABET, USA	150	300 – 750
UV-OSRAM	OSRAM, Germany	18	254

Figure 1: X-ray diffraction (XRD) pattern (a) and Fourier transforms infrared spectroscopy (FTIR) spectrum (b) of g-C_3N_4 nanosheets.
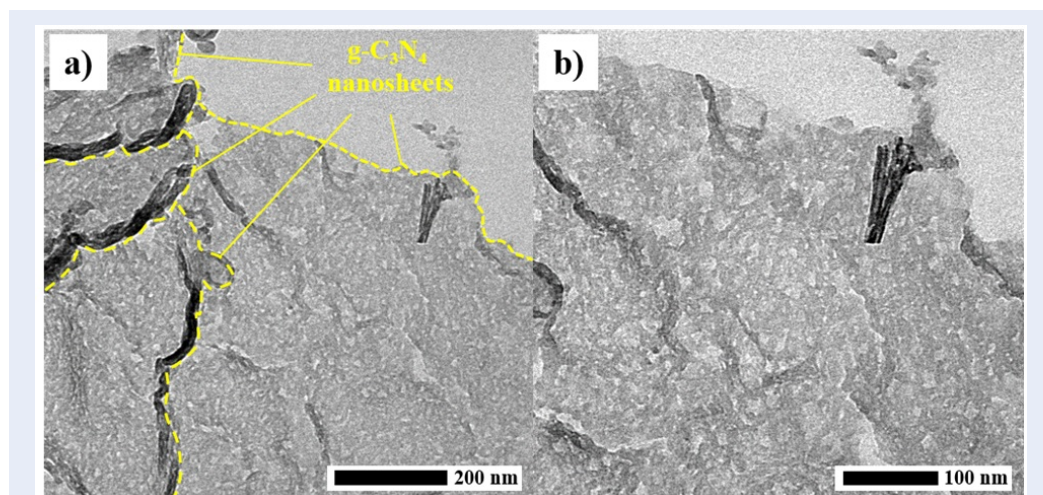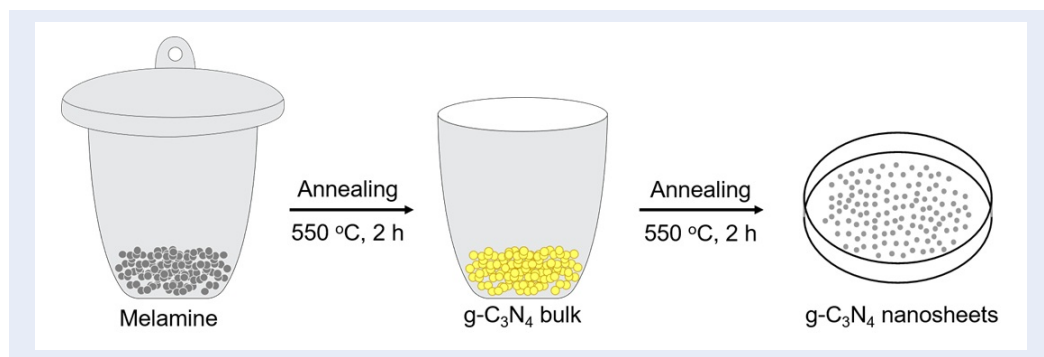

Figure 2: Transmission electron microscopes (TEM) images of g-C3N4 nanosheets at 200 nm (a) and 100 nm scale (b) in the same shooting position.

Scheme 1: **The synthesis process of g-C$_3$N$_4$ nanosheets through a straightforward thermal-exfoliation method by using melamine as the precursor.**
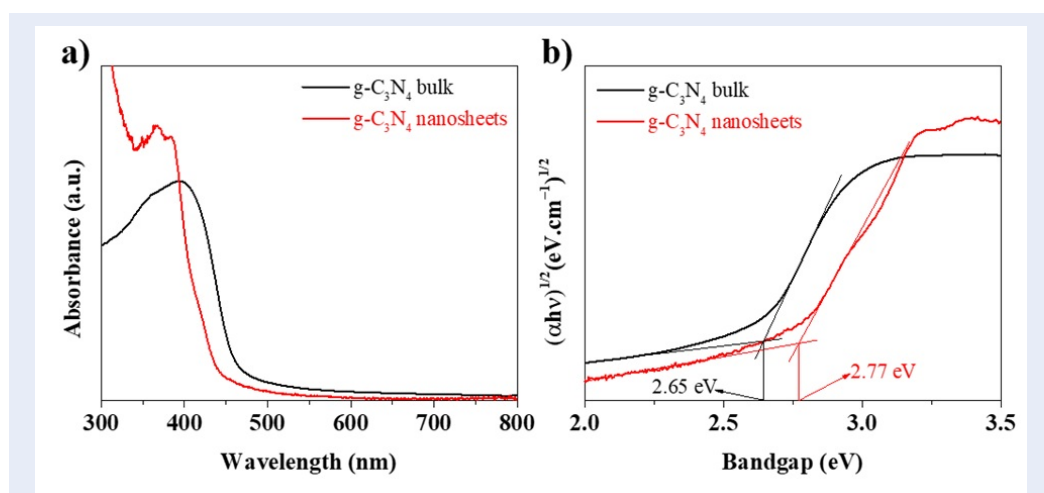

Figure 3: **UV-Vis diffuse reflectance spectroscopy (DRS) spectra (a) and Tauc plots (b) of g-C$_3$N$_4$ bulk and g-C$_3$N$_4$ nanosheets.**

show that g-C$_3$N$_4$ in nanosheets form has a wider bandgap than g-C$_3$N$_4$ in bulk form.

Figure 4a shows the results of the photocatalytic activity of g-C$_3$N$_4$ nanosheets for NO removal under various excitation light sources at a humidity of 70%, consistent with the actual conditions in Vietnam. The results showed that the photocatalytic NO removal efficiency of g-C$_3$N$_4$ nanosheets is the highest at 48.27% for the case of Solar-OSRAM. Meanwhile, the photocatalytic NO removal efficiency of the remaining cases is very low at 37.52%, 8.27%, and 7.26% for Vis-OSRAM, Solar-ABET, and UV-OSRAM, respectively. In addition, the NO$_2$ conversion yield of the Solar-OSRAM case is very low at 9.44%, which is approximately 4.1 times smaller than the NO removal efficiency to green product (NO$_3^-$). Meanwhile, the conversion yield of other cases is very high compared to NO removal to NO$_3^-$ (**Figure 4**b). Moreover, we tabulated key photocatalytic parameters to compare more visually and clearly with recent studies in Table 2. As a result, we can easily see that the performance of g-C$_3$N$_4$ nanosheets with a single component is quite superior to that of the material combinations previously studied for NO degradation. After identifying that the photocatalytic efficiency of g-C$_3$N$_4$ nanosheets is the highest under the solar irradiation, we continue to investigate how the humidity in the atmosphere will affect the photocatalytic process under the solar irradiation, as shown in **Figure 4**c. The results showed that after reducing humidity to 40% and 20%, the photocatalytic efficiency was decreased linearly by 37.52% and 34.18%, respectively. Besides, the NO$_2$ conversion yield was also increased significantly by 11.74% and 13.37%, respectively (**Figure 4**d).
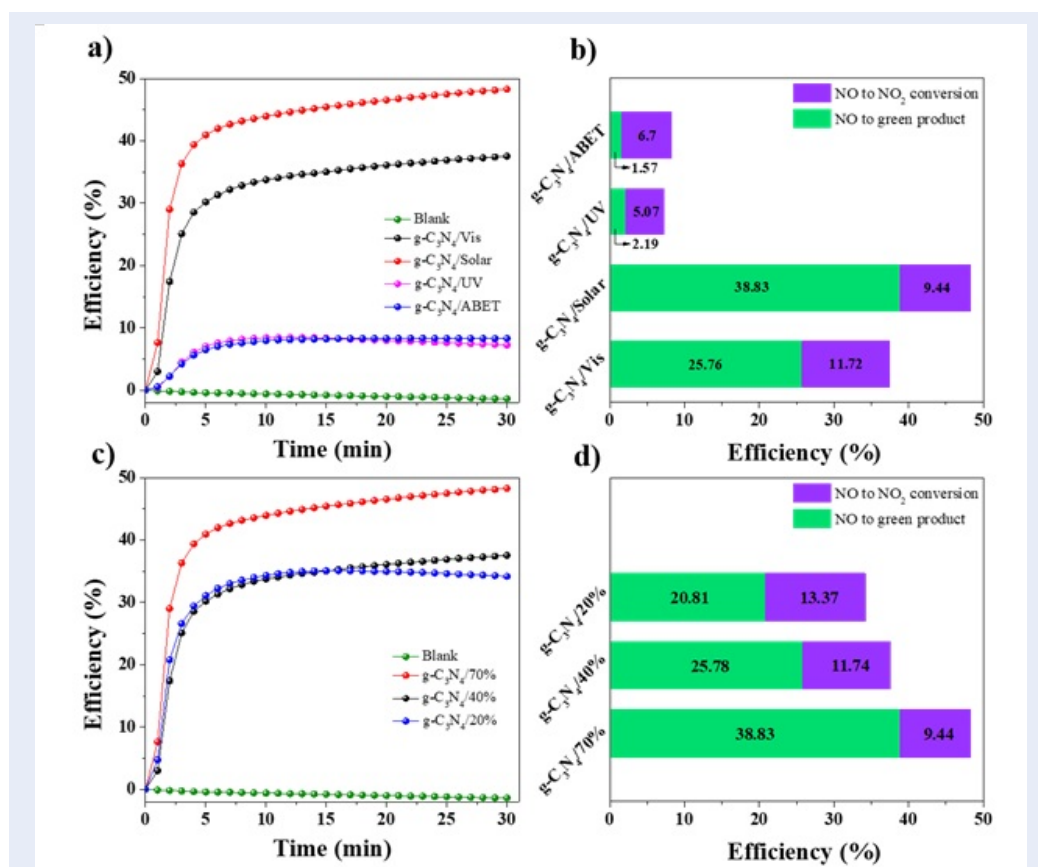
Figure 4: Photocatalytic NO removal efficiency (a), NO removal efficiency, and NO_2 conversion yield (b) in different excitation light sources at 70% humidity, photocatalytic NO removal efficiency (c), NO removal efficiency, and NO_2 conversion yield (d) in different humidity conditions under solar irradiation of g-C_3N_4 nanosheets.

Table 2: A comparison of photocatalysts for the removal of NO

Photocatalyst	NO conc. (ppb)	Exciting light sources	Synthesis method	Efficiency (%)	Ref.
SnO2/PANI	500	OSRAM-300 W	Hydrothermal	14.43	[13]
C-N-S-TiO$_2$	400	Halogen lamp-300W	Hydrothermal	25	[14]
Ag/ZnO	400	Xenon-300W	Microwave-assisted one-pot	55	[15]
g-C$_3$N$_4$	500	OSRAM-300 W	thermal-exfoliation	48.27	This study

To identify the main factor in the photocatalytic process, we conducted photocatalytic trapping tests under solar irradiation conditions at 70% humidity with the presence of KI, $K_2Cr_2O_7$, and BQ to trap factors h^+, e^-, and $\cdot O_2^-$, respectively (**Figure 5**a). The photocatalytic NO removal efficiency was significantly declined by 4.56%, 17.31%, and 35.09% in the existence of KI, $K_2Cr_2O_7$, and BQ, respectively. In addition, we also calculate the reaction kinetic k value to investigate the photocatalytic activity of g-C_3N_4 nanosheets quantitatively. As expected, the results of **Figure 5**b indicate that the k value of the addition of KI is 0.004 min^{-1}, which is much lower than another case (0.123 min^{-1}/pure g-C_3N_4 nanosheets; 0.062 min^{-1}/g-C_3N_4 + $K_2Cr_2O_7$; 0.101 min^{-1}/ g-C_3N_4 + BQ). Moreover, we also investigated the material's durability for practical application by conducting a reusable experiment 5 times of photocatalyst. **Figure 5**c shows that the photocatalytic NO removal efficiency of the g-C_3N_4 nanosheets is still very high at 45.05% after recycling tests. **Figure 5**d presents that the NO_2 conversion yield increases linearly from 9.44% to 16.74%, corresponding to the first to fifth reuse. In addition, we also measure XRD and FTIR of material after recycling tests (**Figure 5**e-f). Surprisingly, all the chemical bonds in the g-C_3N_4 nanosheets still remain after the fifth times reuse and the two diffraction peaks characterize the (100) and (002) planes of g-C_3N_4 are also preserved.

DISCUSSION

Figure 1a shows two typical peaks located at 13.2^o and 27.4^o corresponding to (100) and (002) planes which characterize for in-plane repeated tri-s-triazine units and triazine aromatic systems in g-C_3N_4 structure[16]. In **Figure 1**b, FTIR spectra showed that after undergoing a simple annealing route, melamine precursor formed more chemical bonds in the range from 1700 to 1200 cm^{-1} that characterizes for stretching vibration of C-N heterocycles of g-C_3N_4 nanosheets structure[17]. In addition, the single peak centered at 810 cm^{-1} in the FTIR spectrum of g-C_3N_4 reveals the bending vibrations of the triazine units, which is one of the typical bonds of the g-C_3N_4 matrix[17].

TEM images (**Figure 2**a-b) showed that the morphology of the g-C_3N_4 is a 2D-structured material, including several singly exfoliated sheets. The construction of the 2D-structured nanosheets is due to the formation of strong C-N covalent bonds after undergoing an annealing route to form the nanosheets. Continuing the annealing treatment process, the bond between the nanosheets is the weak physical bond of van der Waals, so they can be easily exfoliated to create a single nanosheet, as shown in the results of the TEM images. Therefore, the morphology of g-C_3N_4 is nanosheets with a large effective area that will be favorable for the photocatalytic process. From the results of modern analytical methods mentioned above (**Figures 1 and 2**), we can conclude that g-C_3N_4 nanosheets material has been successfully synthesized by a simple thermal-exfoliation method.

Figure 3 presents the DRS profile of g-C_3N_4 bulk and g-C_3N_4 nanosheets. This result is perfectly reasonable as there will be a color change from the bright yellow of the bulk to the white color of the sheets. Moreover, the previous publications also showed that when the size of the material is reduced, it leads to a quantum confinement effect that causes the bandgap structure to increase[18,19]. Consequently, the enhancement in the redox ability of the material by increasing the bandgap and thereby facilitating the subsequent photocatalytic reactions.

In **Figure 4**a-b, the results of the photocatalytic NO removal efficiency of g-C_3N_4 nanosheets are highest under solar irradiation at 70% humidity condition. This result can be explained as due to the high power of Osram, 300 W that can provide enough photon energy to activate the maximum photocatalytic reactions of g-C_3N_4 nanosheets. In addition, g-C_3N_4 nanosheets have a relatively narrow bandgap of about 2.7 eV[20]. Consequently, g-C_3N_4 nanosheets can harvest light in both visible and UV regions leading to the photocatalytic NO removal efficiency in the case Solar-OSRAM is the highest. Furthermore, from the results of **Figure 4**c-d, it can be confirmed that the humidity in the air directly influences the photocatalytic efficiency of the material. This phenomenon can be explained by the fact that in the photocatalytic process, the photogenerated hole (h^+) will oxidize the adsorbed H_2O molecules on the photocatalyst surface to form free radical $^\bullet OH$ that contributes to the photocatalytic reactions[5]. Therefore, when the humidity is reduced, the number of H_2O molecules adsorbed on the photocatalyst surface is low, leading to a decrease in the amount of $^\bullet OH$ radicals. Consequently, the photocatalytic efficiency of the material is decreased drastically.

Figure 5a indicated that h^+ plays an essential role in the photocatalytic process, and this result is completely consistent with the results of **Figure 4**c-d. On the other hand, e^- and $^\bullet O_2^-$ also play relative roles in photocatalytic reactions but not as dominant as h^+. In addition, we also calculate the reaction kinetic k value to quantiatively investigate the photocatalytic activity of g-C_3N_4 nanosheets. The reaction kinetic k value is lowest in the case of KI. This means that
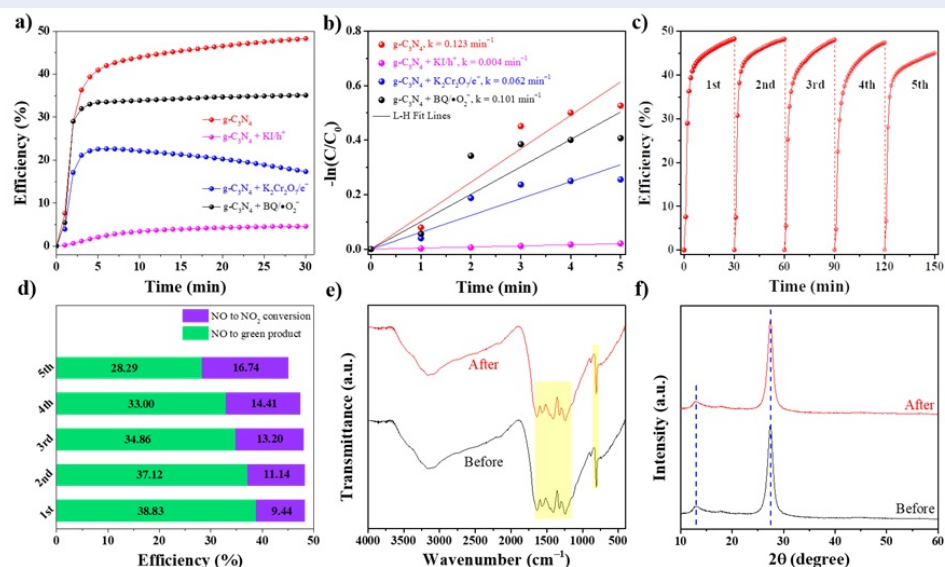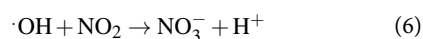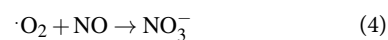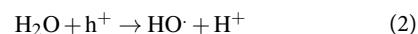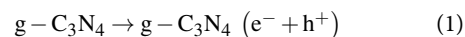
Figure 5: Trapping tests (a), L-H Fit lines (b), recycling test (c), NO removal efficiency and NO_2 conversion yield (d), FTIR spectra (e), and XRD patterns after recycling test of g-C_3N_4 nanosheets.

by trapping h+, the photocatalytic reaction rate has been reduced significantly, or almost none happened. From the results of **Figure 5**a-b, we can solidly confirm that h^+ plays a key role in the photocatalytic process. The results in **Figure 5**c-d can be explained due to the light-shielding effect that reduces the reaction area between the photocatalyst g-C_3N_4 nanosheets and incident light during the photocatalytic process. After each recycling test, the NO gas is decomposed into NO_3^- ions, which will gather on the surface of the photocatalyst, causing the light-shielding effect that prohibits the interaction between the photocatalyst and the light, so decreases the photocatalytic efficiency [5]. From the results of **Figure 5**c-f, we can confirm that the g-C_3N_4 nanosheets have very high durability and can be put into practical application for photocatalytic NO removal at a high concentration level with many times reuse.

From the analyzed results above, we propose a photocatalytic mechanism model for the 2D-structured g-C_3N_4 nanosheets under solar light at 70% humidity by the following equations (**Figure 6**). When sunlight is irradiated with an incident wavelength greater than the energy of the bandgap, electrons (e^-) will move from the valence band (VB) to the conduction band (CB), leaving a hole (h^+) (**Equation (1)**). Therefore, h^+ will be abundant in VB, and e^- will be rich in CB. Then, a few e^- and h^+ will migrate to the surface of the photocatalyst and react with the

adsorbed O_2 and H_2O molecules on the photocatalyst surface (**Equations (2) and (3)**). The h^+ oxidizes H_2O molecules to $^\bullet OH$ radicals. Meanwhile, e^- will reduce O_2 molecules to $^\bullet O_2^-$ radicals. These free radicals with high redox activity will decompose NO gas into NO_3^-, which is a less toxic product than the original NO gas (**Equations (4), (5) and (6)**).

$$g - C_3N_4 \rightarrow g - C_3N_4 \ (e^- + h^+) \tag{1}$$

$$H_2O + h^+ \rightarrow HO\cdot + H^+ \tag{2}$$

$$O_2 + e^- \rightarrow \cdot O_2^- \tag{3}$$

$$\cdot O_2 + NO \rightarrow NO_3^- \tag{4}$$

$$\cdot OH + NO \rightarrow NO_2 + H^+ \tag{5}$$

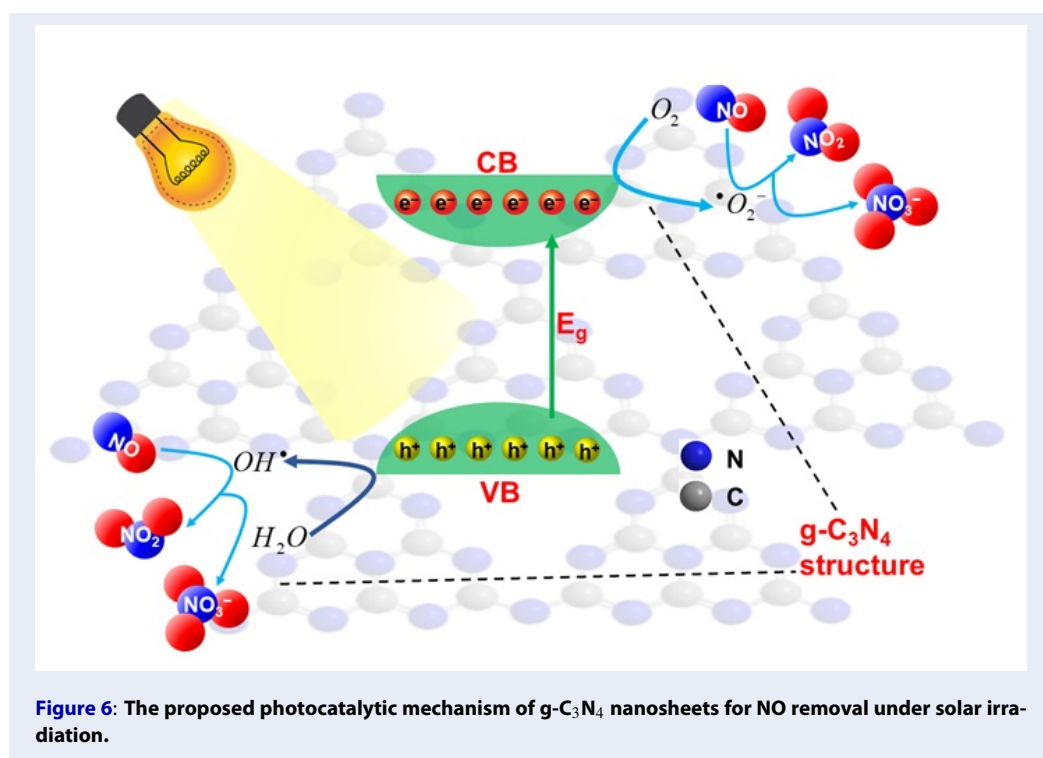$$\cdot OH + NO_2 \rightarrow NO_3^- + H^+ \tag{6}$$

Figure 6: **The proposed photocatalytic mechanism of g-C$_3$N$_4$ nanosheets for NO removal under solar irradiation.**

CONCLUSIONS

In brief, we have successfully synthesized 2D-structured g-C$_3$N$_4$ nanosheets by undergoing a simple thermal-exfoliation method. This is evidenced by the results of XRD, FTIR, TEM, and DRS results. The as-synthesized g-C$_3$N$_4$ nanosheets achieve a very high photocatalytic NO removal at 48.27% under solar irradiation at 70% humidity thanks to the benefits of large specific surface area and narrow bandgap of the material. Moreover, the NO$_2$ conversion yield is very low, only 9.44%, compared to 38.83% of the decomposition efficiency NO to NO$_3^-$ ions. In addition, we also indicated that the h$^+$ plays the most critical role in the photocatalytic reaction by trapping tests. Besides, the photocatalytic NO removal efficiency still reaches 45.03% after fifth times reuse. These results of XRD pattern and FTIR spectrum of photocatalyst after recycling tests still show all the characteristic diffraction peaks and typical chemical bonds in the g-C$_3$N$_4$ nanosheets original state of the photocatalyst before recycling test. From the analysis results above, we can confirm that g-C$_3$N$_4$ nanosheets possess a very high practical application potential for decomposing NO gas at high concentrations under solar irradiation.

ABBREVIATIONS

g-C$_3$N$_4$: graphitic carbon nitride

2D: two dimensions
XRD: X-ray diffraction
FTIR: Fourier transforms infrared spectroscopy
TEM: Transmission electron microscopes
DRS: UV-Vis diffuse reflectance spectroscopy
VB: valence band
CB: conduction band
h$^+$: hole
e$^-$: electron

ACKNOWLEDGEMENTS

AUTHORS CONTRIBUTION

Tran Hoang The Vinh: Investigation, Writing - Original draft preparation;
Huynh Cam Tu: Formal analysis;
Pham Van Viet: Writing — Review & Editing, Supervision, Funding acquisition.

CONFLICT OF INTEREST

The authors declare that they have no known competing financial interests or personal relationships that could have appeared to influence the work reported in this paper.

REFERENCES

1. Anenberg SC, Miller J, Minjares R, Du L, Henze DK, Lacey F, et al. Impacts and mitigation of excess diesel-related NOx emissions in 11 major vehicle markets. Nature. 2017;545(7655):467-71;PMID: 28505629. Available from: https://doi.org/10.1038/nature22086.

2. Gomez-Garcia MA, Pitchon V, Kiennemann A. Pollution by nitrogen oxides: an approach to NO(x) abatement by using sorbing catalytic materials. Environ Int. 2005;31(3):445-67;PMID: 15734196. Available from: https://doi.org/10.1016/j.envint.2004.09.006.

3. Todorova N, Giannakopoulou T, Karapati S, Petridis D, Vaimakis T, Trapalis C. Composite TiO2/clays materials for photocatalytic NOx oxidation. Applied Surface Science. 2014;319:113-20;Available from: https://doi.org/10.1016/j.apsusc.2014.07.020.

4. Rokni E, Ren X, Panahi A, Levendis YA. Emissions of SO2, NOx, CO2, and HCl from Co-firing of coals with raw and torrefied biomass fuels. Fuel. 2018;211:363-74;Available from: https://doi.org/10.1016/j.fuel.2017.09.049.

5. Huy TH, Bui DP, Kang F, Wang YF, Liu SH, Thi CM, et al. SnO2/TiO2 nanotube heterojunction: The first investigation of NO degradation by visible light-driven photocatalysis. Chemosphere. 2019;215:323-32;PMID: 30321811. Available from: https://doi.org/10.1016/j.chemosphere.2018.10.033.

6. Loeb SK, Alvarez PJJ, Brame JA, Cates EL, Choi W, Crittenden J, et al. The Technology Horizon for Photocatalytic Water Treatment: Sunrise or Sunset? Environ Sci Technol. 2019;53(6):2937-47;PMID: 30576114. Available from: https://doi.org/10.1021/acs.est.8b05041.

7. Viet PV, Huy TH, You S-J, Hieu LV, Thi CM. Hydrothermal synthesis, characterization, and photocatalytic activity of silicon doped TiO2 nanotubes. Superlattices and Microstructures. 2018;123:447-55;Available from: https://doi.org/10.1016/j.spmi.2018.09.035.

8. Ha LPP, Vinh THT, Thuy NTB, Thi CM, Viet PV. Visible-light-driven photocatalysis of anisotropic silver nanoparticles decorated on ZnO nanorods: Synthesis and characterizations. Journal of Environmental Chemical Engineering. 2021;9(2);Available from: https://doi.org/10.1016/j.jece.2021.105103.

9. Bui DP, Nguyen MT, Tran HH, You S-J, Wang Y-F, Van Viet P. Green synthesis of Ag@SnO2 nanocomposites for enhancing photocatalysis of nitrogen monoxide removal under solar light irradiation. Catalysis Communications. 2020;136;Available from: https://doi.org/10.1016/j.catcom.2019.105902.

10. Fu J, Yu J, Jiang C, Cheng B. g-C3N4-Based Heterostructured Photocatalysts. Advanced Energy Materials. 2018;8(3);Available from: https://doi.org/10.1002/aenm.201701503.

11. Cao S, Low J, Yu J, Jaroniec M. Polymeric photocatalysts based on graphitic carbon nitride. Adv Mater. 2015;27(13):2150-76;PMID: 25704586. Available from: https://doi.org/10.1002/adma.201500033.

12. Hoang TVT, Minh TC, Van VP. Enhancing photocatalysis of NO gas degradation over g-C3N4 modified α-Bi2O3 microrods composites under visible light. Materials Letters. 2020;281;Available from: https://doi.org/10.1016/j.matlet.2020.128637.

13. Bui PD, Tran HH, Kang F, Wang Y-F, Cao TM, You S-J, et al. Insight into the Photocatalytic Mechanism of Tin Dioxide/Polyaniline Nanocomposites for NO Degradation under Solar Light. ACS Applied Nano Materials. 2018;1(10):5786-94;Available from: https://doi.org/10.1021/acsanm.8b01445.

14. Wang Y, Huang Y, Ho W, Zhang L, Zou Z, Lee S. Biomolecule-controlled hydrothermal synthesis of C-N-S-tridoped TiO2 nanocrystalline photocatalysts for NO removal under simulated solar light irradiation. J Hazard Mater. 2009;169(1-3):77-87;PMID: 19398265. Available from: https://doi.org/10.1016/j.jhazmat.2009.03.071.

15. Liu H, Liu H, Yang J, Zhai H, Liu X, Jia H. Microwave-assisted one-pot synthesis of Ag decorated flower-like ZnO composites photocatalysts for dye degradation and NO removal. Ceramics International. 2019;45(16):20133-40;Available from: https://doi.org/10.1016/j.ceramint.2019.06.279.

16. Dong F, Wu L, Sun Y, Fu M, Wu Z, Lee SC. Efficient synthesis of polymeric g-C3N4 layered materials as novel efficient visible light driven photocatalysts. Journal of Materials Chemistry. 2011;21(39);Available from: https://doi.org/10.1039/c1jm12844b.

17. Zhang W, Zhou L, Deng H. Ag modified g-C3N4 composites with enhanced visible-light photocatalytic activity for diclofenac degradation. Journal of Molecular Catalysis A: Chemical. 2016;423:270-6;Available from: https://doi.org/10.1016/j.molcata.2016.07.021.

18. Dong F, Li Y, Wang Z, Ho W-K. Enhanced visible light photocatalytic activity and oxidation ability of porous graphene-like g-C3N4 nanosheets via thermal exfoliation. Applied Surface Science. 2015;358:393-403;Available from: https://doi.org/10.1016/j.apsusc.2015.04.034.

19. Li K, Huang Z, Zhu S, Luo S, Yan L, Dai Y, et al. Removal of Cr(VI) from water by a biochar-coupled g-C3N4 nanosheets composite and performance of a recycled photocatalyst in single and combined pollution systems. Applied Catalysis B: Environmental. 2019;243:386-96;Available from: https://doi.org/10.1016/j.apcatb.2018.10.052.

20. Mamba G, Mishra AK. Graphitic carbon nitride (g-C3N4) nanocomposites: A new and exciting generation of visible light driven photocatalysts for environmental pollution remediation. Applied Catalysis B: Environmental. 2016;198:347-77;Available from: https://doi.org/10.1016/j.apcatb.2016.05.052.